HEMODYNAMIC RESPONSES TO THERMAL STIMULATION IN THE PREFRONTAL CORTEX OF THE BRAIN MEASURED BY FNIRS

By

KOUMUDI CHARI

Presented to the Faculty of the Graduate School Of

The University of Texas at Arlington in Partial Fulfillment

Of the Requirements

For the Degree of

MASTER OF SCIENCE IN BIOMEDICAL ENGINEERING

THE UNIVERSITY OF TEXAS AT ARLINGTON

AUGUST 2015

Acknowledgements

I sincerely thank my supervising professor, Dr. Hanli Liu for her guidance and unwavering support throughout the course of research. I would also like to thank my committee members Dr.Peng and Dr. Robert Gatchel.

I would like to mention special thanks to my mentor, Mr. Amarnath, for patiently supporting and directing me towards the accomplishment of the project goal. I would also like to thank my colleagues and friends, who helped me by volunteering for my experimentation work.

I would also like to acknowledge the financial support provided by Dr. Liu. And most importantly, I would thank my family and friends for their love and support throughout the master's degree.

August 3 2015

Abstract

HEMODYNAMIC RESPONSES TO THERMAL STIMULATION IN THE PRE-FRONTAL CORTEX OF THE BRAIN MEASURED BY FNIRS

Koumudi Chari, M.S.

The University of Texas at Arlington, 2015

Supervising Professor: Hanli Liu

Although FMRI has marked its importance in the neurological research by understanding the brain activities, FNIRS has also set a new standard in the brain imaging study research with non-invasive and easy to use technology. FNIRS is a portable, inexpensive optical imaging method that measures the changes in the oxygenated and de-oxygenated hemoglobin of the brain that results from the neurological activity. In this study, FNIRS has been used to study the pain processing in humans by measuring the pre-frontal cortex area of the brain. Eight (n=8) healthy subjects were induced with pain using a thermal stimulator device with temperatures ranging from 45 to 47°C and their temporal profiles of the brain activity were analyzed to see which part of the pre-frontal cortex showed changes in the hemodynamic response. Apart from this, first 2 blocks and the last 2 blocks of the experimental protocol were compared to see if there were any symptoms of pain habituation due to repeated painful stimuli for six times. Significant deactivations were observed at the time of the painful stimuli which covered areas of the pain matrix including dorsolateral pre-frontal cortex (BA 9 and 46), frontopolar cortex (BA10) etc. Activations were found during the recovery phase in the areas of dorsolateral prefrontal cortex (BA 9 and 46), frontopolar area (BA 10) and parts of broca area. On the other hand, Dorsolateral pre-frontal cortex and anterior pre-frontal cortex (BA 9,10,46) showed less deactivation in the first 2 blocks than the last 2 blocks

and hence, it was also proved that repeated painful stimuli leads to adaptation of the signal.

Table of Contents

List of Illustrations

List of Tables

Chapter 1

Introduction

1.1 Functional Near infrared Spectroscopy (FNIRS)

1.1.1 Overview

Near infrared spectroscopy is becoming increasingly popular in the recent times for studying the activity in the human brain by using the principle of Modified Beer- Lamberts law. Although FMRI has proved its dominance in the field of in vivo imaging of the human brain study, FNIRS has also marked its significance in various domains. FNIRS has been used to study neurological (Alzheimer's disease, Parkinson's disease, epilepsy, traumatic brain injury) and psychiatric disorders (schizophrenia, mood disorders, anxiety disorders) [25]. It has also been used to study the cognitive functioning of the brain like information processing speed of an individual, problem solving, attention control, working memory and the general functioning of the brain [17].

A basic multi-channel FNIRS system consists of LED or laser as sources and photo diode detectors, a digital signal processing board for real time data acquisition and demodulation of the signals and a computer for display. The optode channels probe geometry is designed according to the requirements of the study. Changes in the blood flow, blood volume and oxygenation due to cognitive functioning of the brain enables FNIRS and FMRI to measure the brain activity. FMRI is known to measure the Blood Oxygenation Level Dependent response (BOLD) that results from de- oxygenated hemoglobin. FMRI has become a dominant imaging method due to its high spatial resolution, but it also has many disadvantages.

On the other hand, FNIRS is known to measure the changes in the oxy and de-oxy hemoglobin contents in the brain by using near-infra red light. It has several advantages over FMRI that include better temporal resolution, non-invasive and easy to use, flexible technology. Apart from this, FNIRS can be used with ease when performing complex experimental paradigms such as measurement of end tidal CO2 simultaneously while measuring the brain signals, face-to-face communication with the subjects, pain stimulation, etc. In such cases, FMRI can be proved challenging due to its complex and bulky machinery. Other disadvantages of FMRI over FNIRS include, biological harm due to powerful magnetic fields, head motion, probes positioning, etc. Also, the presence of metal in the body (such as pacemakers or other implants) can be a safety hazard while performing an FMRI scan.

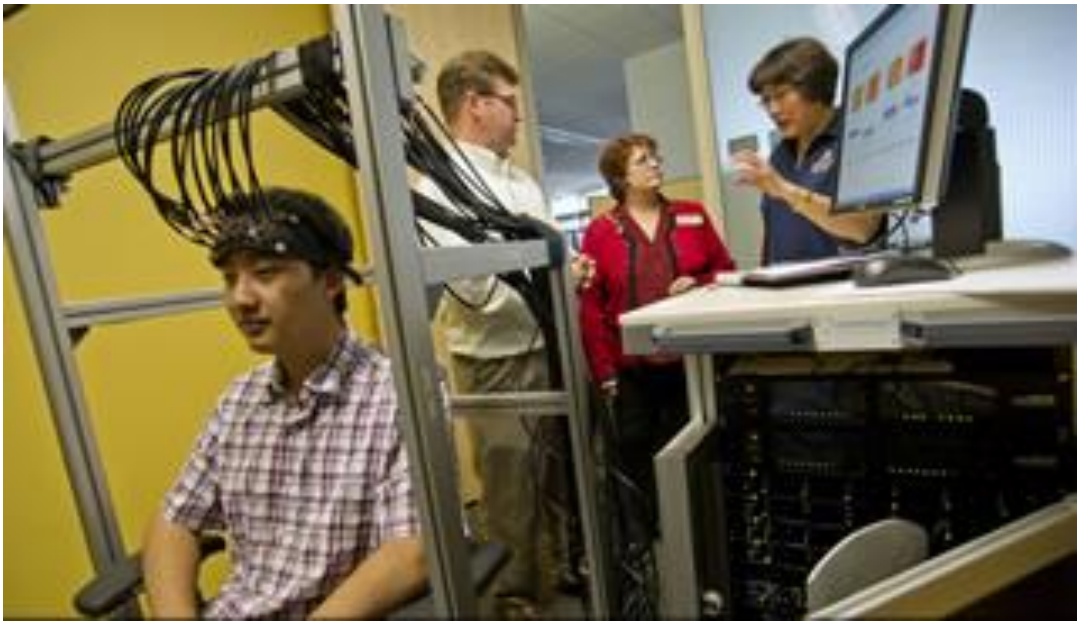

Figure 1.1 shows the setup of an FNIRS machine

[http://www.uta.edu/midic/executive-committee.php]

Although FNIRS has many advantages, it has many limitations like poor spatial resolution, low Signal-to-Noise ratio compared to FMRI. The main drawback of using FNIRS over FMRI is inability to measure the deeper layers of the brain.

1.1.2 Principle of operation:

Functional Near Infrared Spectroscopy is a non-invasive optical imaging method that uses near infrared light to measure the oxy and de-oxy hemoglobin concentrations from the brain that results from neuronal activation. The wavelength of the near infrared light ranges from 600-900 ηm in the electromagnetic spectrum just beyond the visible light.

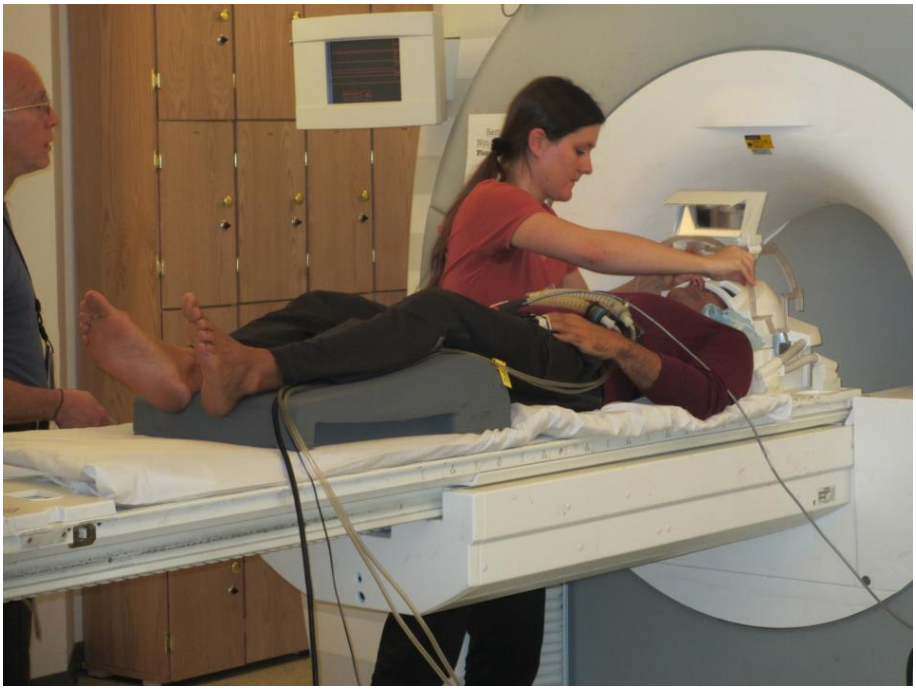

Figure 1.2 shows a complex set up and experimentation of the FMRI technology [http://cns.bu.edu/~gdesbord/research.html]

The attenuation co-efficient of HbO and Hb are too large for the wavelengths shorter than 650nm. This implies that the radiation having a wavelength less than 650nm

will be completely absorbed by the biological tissue. On the other hand, the extinction co-efficient of water increases above 900nm causing light to get fully absorbed beyond this

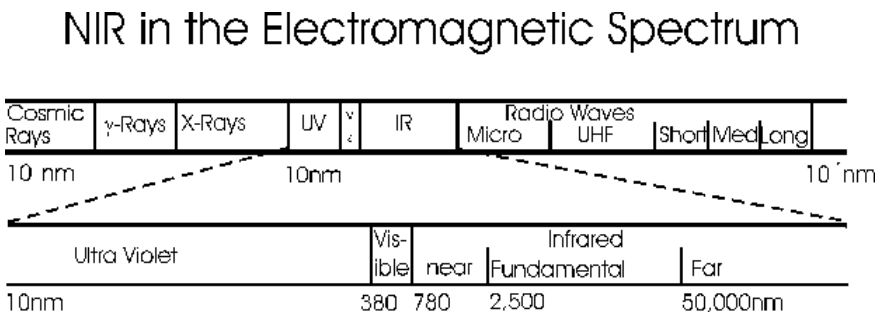

Figure 1.3 shows the representation of an Electromagnetic spectrum

[https://www.impublications.com/content/introduction-near-infrared-nir-spectroscopy]

Wavelength. Therefore, the favorable range for measuring the properties of biological tissue ranges from 650nm to 900 nm wherein light can penetrate at maximum depth. This particular range is known as ‘optical window’ since most of the biological tissue chromophores are relatively transparent to light in this range. This is due to the fact that absorption of light into the tissue by its physiological chromophores like oxy hemoglobin and de-oxy hemoglobin is less, thereby permitting the light to penetrate deeper into the tissue.

1.1.2.1 Beer-Lambert’s Law:

In a homogenous medium, it is assumed that light travels in a straight line, until it interacts with other medium or particle. But, on the other hand, when light travels through a dispersing medium, it undergoes attenuation and scattering. Similarly, when light enters into the tissue, part of it is absorbed and part of it is scattered.

Absorption is quantified using the term absorption co-efficient denoted by μa. absorption co-efficient is determined by how far the light can penetrate into the material before it is absorbed.

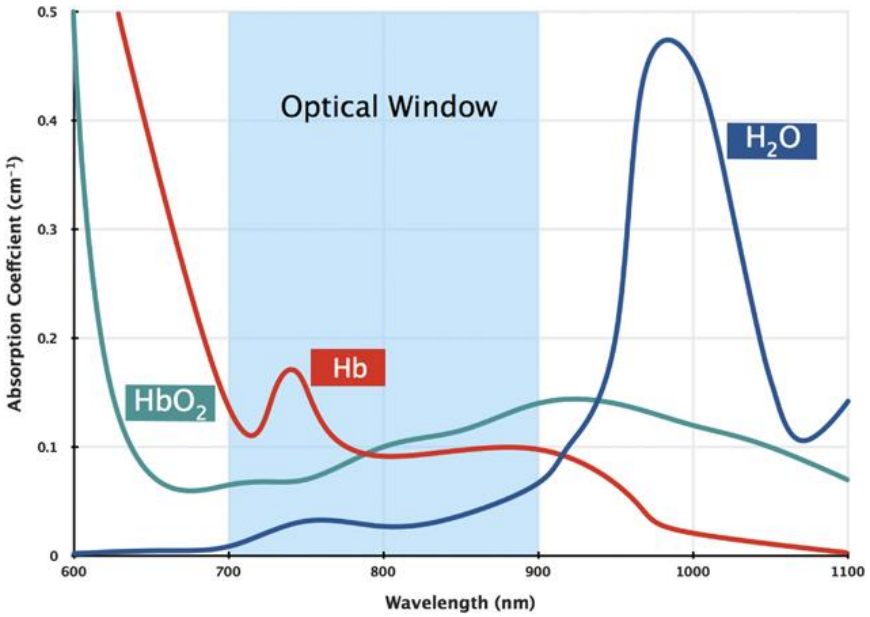

Figure 1.4 shows Absorption Spectra of HbO, Hb, and Water

[http://www.nature.com/icb/journal/v88/n4/fig_tab/icb2009116f1.html]

$$\mu a = 2.3 * € * C$$

where, € is the wavelength dependent molar absorptivity co-efficient i.e, the measure of absorption of light in a medium, C is the concentration of the absorbing substance.

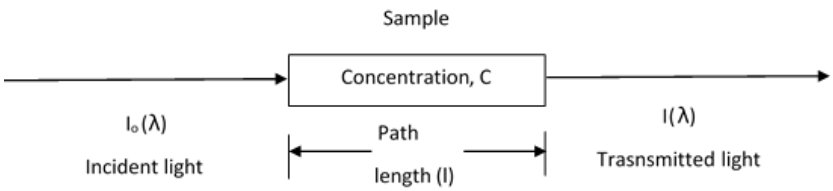

Figure 1.5 represents Absorption coefficient

Similarly, scattering in optically thick media can be characterized by two parameters, scattering anisotropy (g) and scattering co-efficient (μs).

a) Scattering anisotropy: It represents the mean cosine of scattering angle between the incident and scattered light.

i.e. $g = < \cos\theta >$

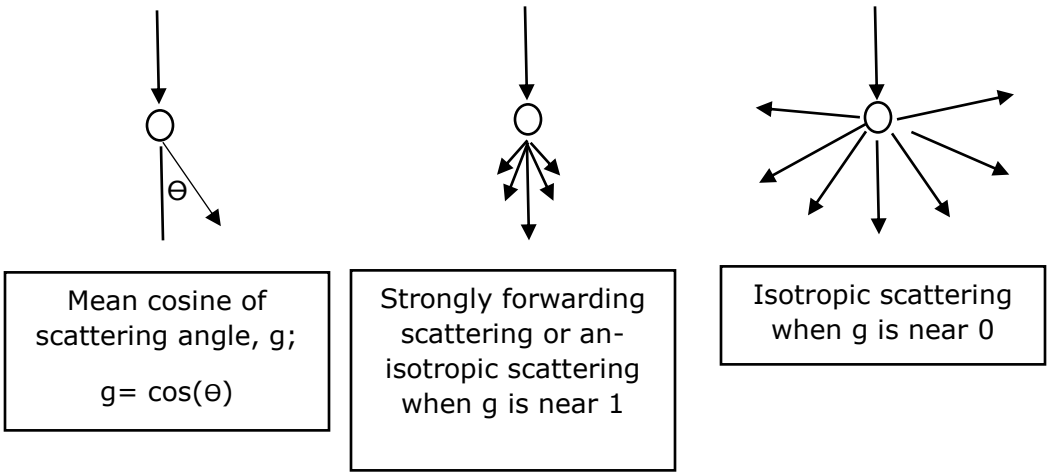

Figure 1.6 Shows that when g=1 we have strong forward scattering, and when g=0, we have isotropic scattering since Θ = 90°

b) Scattering co-efficient (μ_s): It represents the mean scattering length or mean free path between two scattering events A & B.

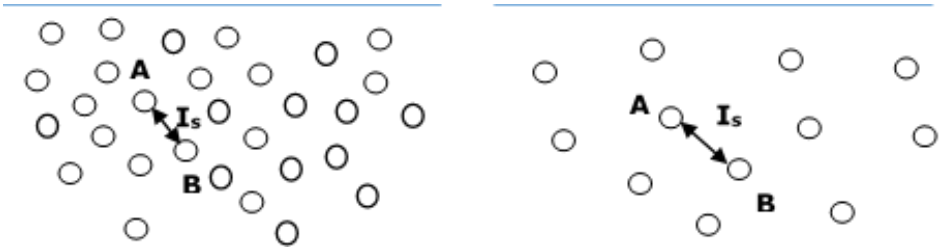

Figure 1.7 shows a denser scattering medium has shorter l_s and larger μ_s value

$$l_s = \frac{1}{\mu_s}$$

c) Reduced Scattering co-efficient (μ_s'): It is the measure of mean free path travelled between two isotropic scatterers A& B.

$$\mu_s' = \mu_s(1 - g) \text{ in } cm^{-1}$$

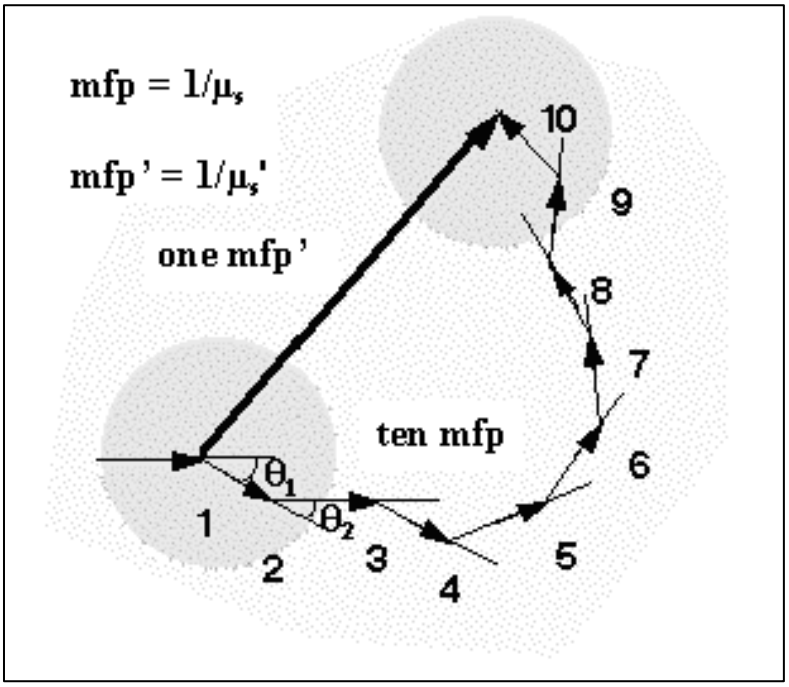

Figure 1.8 shows Reduced Scattering Coefficient

In the FNIRS, when the light passes into the tissue through a source and it diffuses back through the detector, the change in the light absorption is represented as Delta Optical Density (ΔOD). This relationship between the change in optical density and concentration of the physiological chromophores is given by

$$\Delta OD ij^{\lambda} = Lij^{\lambda}\left(\epsilon^{\lambda}_{HbR}\ \Delta[HbR] + \epsilon^{\lambda}_{HbO2}\ \Delta[HbO2]\right);$$

where Є is the wavelength dependent molar absorptivity co-efficient for hemoglobin species. L_{ij} is the mean path length between the source i to detector j. However, the propagation of light through the biological tissue follows a scattering path, rather than following a straight path, the beers lamberts law has to be modified to compensate for the additional distance that it travels while scattering. The path length that the light uses to travel from the source to the detector can be calculated as L = d * DPF, where d is the distance between the source and detector and DPF is the differential path factor. Using the diffusion equation for modeling light transport through a homogeneous semi-infinite medium, it has been proved that the DPF depends on μa(λ), the reduced scattering coefficient μ′s(λ), and d [1].

According the Modified Beer Lambert's Law, change in optical density is given by the equation:

ΔOD = log (Io/I) =εcL = kc ..... (1.1)

where

ΔOD = change in optical density,

Io = Light intensity before the change of concentration,

I = Light intensity after the change of concentration,

ε = extinction coefficient of absorbing tissue,

L = path length through the tissue,

k = proportionality constant.

On the other hand, the net absorption change at each wavelength due to changes in hemoglobin concentration is specified by the following equation

$$\Delta ODij^{\lambda} = Lij^{\lambda}\ DPE^{\lambda}\left(\in_{HbR}^{\lambda} \Delta[HbR] + \in_{HbO2}^{\lambda} \Delta[HbO2]\right);$$

In the above equation, the term DPF (differential path-length factor) has been added to account for differences between the linear distance between the source and detector pair (Lij) and the true effective mean path length that light travels as it scatters through the tissue.

1.1.3 Brain physiology

The transmittance measurements using the NIR radiation can be used to create images of the brain physiology by measuring the cerebral blood flow. Human brain undergoes many physiological changes when performing any type of task. These changes cause certain metabolic requirements in the brain. The oxygen content of the blood tends to increase in certain areas of the brain depending upon the activation. This oxygen metabolism causes the HbO and HbR content to change and also results in decrease in tissue oxygenation which is counteracted by increase in O2 supply leading to increase in CBV and CBF which can be captured using FNIRS. This is called as neurovascular coupling. The CBF and oxygen metabolism increases not only to counteract the effect of tissue oxygenation, but also to oxygenate hemoglobin.

Chapter 2

Introduction to Pain study

2.1 Overview of Pain

Pain is defined as a “complex constellation of unpleasant sensory, emotional and cognitive experiences provoked by real or perceived tissue damage and manifested by certain autonomic, psychological, and behavioral reactions” [2]. Pain is an important communication tool for the human body system because if the person cannot perceive pain due to hereditary neuropathies, he is more likely to fall prey to unrealized infections and may end up having a short life span [3]. But at the same time, pain is also an unpleasant sensory and emotional experience. It has multiple causes, and people respond to it in multiple and individual ways depending upon the intensity, type and duration. pain can be experienced and felt in a wide variety of ways that includes ancinating, stabbing, or pricking, burning, throbbing, cramping, and aching [4]. Nociceptors are specialized peripheral sensory neurons that notify the human brain about potentially harmful stimuli hurting and damaging the skin by detecting the increase in temperature, pressure or injurious chemicals.

2.2 Classification of pain

Pain can be categorized in several ways. One way of pain classification is acute and chronic pain. Acute pain is caused by damage to tissue such as bone, muscle, or organs and people often experience anxiety and emotional stress at the onset of it. It is known to happen suddenly and stays for a short period of time. On the other hand, chronic pain is usually associated with a long-term illness, such as pain of arthritis or tumor invading soft tissues and is resistant to medical treatment. Sprains and strain are examples of mild chronic pain. The other common types of pain include nociceptive pain, neuropathic pain

and inflammable pain. Nociceptive pain is the pain that represents the response to tissue injury such as skin, muscles, visceral organs, joints, tendons, or bones. Few examples include joint pain, myofascial pain. Neuropathic pain is caused by a primary lesion or disease in the somatosensory nervous system. Neuropathic pain examples include diabetic neuropathy, spinal cord injury pain, post-amputation pain. Inflammatory pain results when nociceptive pain pathway activates and sensitizes a variety of mediators released at a site of tissue inflammation. Examples include appendicitis, rheumatoid arthritis, and inflammatory bowel disease.

2.2.1 Nociceptors

Nociception is defined as the neural process of encoding and processing noxious stimuli. There are distinct classes of nociceptors that are activated by noxious stimuli. The stimuli include, intense pressure, harmful chemicals causing tissue damage and temperatures ranging from 40-45°C or less than 15°C.

The perception of pain, however, is not only dependent on the nociception activity but it is also dependent on peripheral information and frequency of action potentials, temporal summation of pre and post-synaptic signals and central influences [5]. The axons associated with the nociceptors are divided into two types:

Aδ group and C fiber group. Aδ group of nociceptors are myelinated axons that respond either to dangerously intense mechanical or to mechanothermal stimuli, and have receptive fields that consist of clusters of sensitive spots. They conduct at velocities of 20m/s. C fiber group of nociceptors are unmyelinated axons that respond to thermal, mechanical, and chemical stimuli. The conduct at velocities less than 2m/s [2]. Find the reference. Thermal nociceptors respond to noxious heat or cold at various temperatures, mechanical deformation, incision at the skin surface or excess pressure activates the

Mechanical nociceptor. The TRP channels in the chemical nociceptors respond to wide variety of chemicals like Capsiacin, acrolein, cigarette smoke.

2.3 Conduction of pain

A nerve cell that responds to the noxious stimuli at its periphery and sends signals to the spinal cord and the brain is called as a nociceptor. These signals should be above the threshold for an action potential to reach the central nervous system. When the action potential keeps inducing and forms a train of events, pain alerts the human body. The nociceptor responds to thermal, chemical and mechanical features of the environment depending upon the ion channels it releases at the periphery of the nerve cell. This feature of the nociceptor is called as the 'specificity of the nociceptor '.

The nociceptive fibers that travel back to the spinal cord after sending information to the brain are called Afferent nociceptive fibers. These nociceptors located in the periphery form the synapses in the dorsal horn are called the first order neuron. The cells in the dorsal horn are divided into physiologically distinct layers called laminae. Synapses of different fiber types are formed in different layers. Glutamate or substance P are the neurotransmitters that are released by the nerve fibers. Aδ fibers, C fibers and Aβ fibers connect to form synapses with laminae I and V, lamina II and Lamina I, III and V respectively. After that, the first order nociceptive project to second order neurons thatcross the midline at the anterior white commissure. The dorsal column medial-lemniscal system and theanterolateral system are the two pathways through which second order neurons send their information to the thalamus. The non-painful sensation uses the dorsal system pathway whereas the painful sensation uses the lateral system. , the information processing happens in the ventral posterior nucleus and then is sent to the cerebral cortex in the brain via fibers in the posterior limb of the internal capsule.

2.4 Aim of Pain study

Pain is an experience that is evoked by a harmful stimulus which directs your attention towards a danger and holds you attention. Insensitivity to pain can be dangerous and may also prove fatal at times. Pain has proved to be an astounding burden in the United States Of America. According to Relieving Pain in America: A Blueprint for Transforming Prevention, Care, Education, and Research, every year the people of United States spend around $560 billion to $635 billion to treat pain according to a recent report [6]. Pain plays a very major role in the everyday activities and general functioning of a person's life. Patients suffering from acute pain and chronic pain have been found to report impairments in attention control, working memory, mental flexibility, problem solving, and information processing speed. Acute and chronic pain are also associated with increased depression, anxiety, fear, and anger [7]. But, on the other hand, there is no accurate way of telling how much pain a person is going through. To determine the intensity of pain, it is necessary to locate pain precisely, and to assess the effect of pain on someone's life. Apart from this, there is a need of a proper assessment tool to objectively measure the amount of pain, so that the clinician can prescribe adequate dosage to relieve pain. Although defining pain as sharp or dull, constant or intermittent, burning or aching may give the best clues to the cause of pain, a proper test for pain assessment using a medical device would be a very useful tool in diagnosing and treating pain.

Numerous technologies have been used indirectly to find the cause and effect of pain, but so far, no accurate assessment tool has been found to measure pain objectively. A few of them include, a musculoskeletal and neurological examination that measure the movement, reflexes, balance and co-ordination of the nerve and muscle, laboratory tests that help the physician diagnose infection, cancer and other factors influencing pain,

electromyography, nerve conduction studies and evoked potential studies have been used to check the proper functioning of the nerves and to evaluate muscle symptoms resulting from a disease or injury. Using Functional magnetic resonance imaging, cerebral processing of the experience of pain involved different networks like cerebral cortex activity in prefrontal cortex (PFC) reflects attentional and memory networks activated by noxious stimulation [8], primary and secondary somatosensory cortex, anterior cingulate cortex(ACC) participates in both affective and attentional concomitants of pain sensation [9]. Recent studies using FMRI have been used to demonstrate the feasibility of discriminating painful from non-painful stimulations [10].

But due to the challenges faced by FMRI like poor temporal resolution, complex machinery, FNIRS an optical brain imaging method has been used in the recent decades for carrying out neuroimaging studies of the brain because of its flexibility of carrying out measurements without constraining patients body or head [11]. FNIRS detects the changes in oxy and de-oxy hemoglobin concentration as a result of neuronal activity. FNIRS has been known to find brain activations similar to FMRI during pain measurements. Mechanical pain stimulation in the lower back elicited deactivation in pre-frontal cortex area of the brain [11]. In the University of texas at Arlington, a FNIRS based study was performed by inducing high pain (HP) and low pain (LP) into the subjects' TMJ (temporo mandibular joint) by using a thermal stimulator machine.

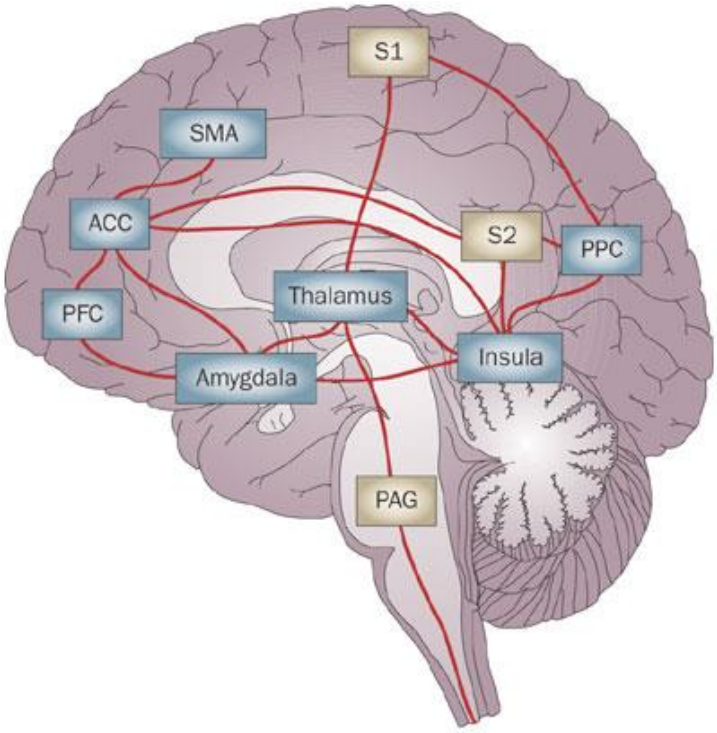

Figure 2.1 shows the areas of the brain that show significant hemodynamic changes in the brain called as the pain matrix [http://www.nature.com/nrneurol/journal/v5/n4/fig_tab/nrneurol.2009.28_F1.html]

HbO signals showed an initial activation in the frontal cortex during the high-pain stimulation phase, followed by deactivation during the recovery phase before returning to the baseline [10].

The aim of the present study was to investigate the effect of thermal pain on the pre-frontal cortex area of the brain using FNIRS with short-separation measurements and to analyze the pain temporal profile for any habituation symptoms. The inexpensive, non-invasive, brain imaging modality may help us lead to a better understanding of pain processing at the cortical regions induced by acute pain. The long term goal of this experiment is to use FNIRS as a pain assessment tool to study the intensity of pain suffered by the patient so that the clinician can decide on the right mode and amount of

treatment and also see if there are any differences in the brain activations and hemodynamic responses between healthy and pain patients. The pain matrix consists of various sub-cortical and cortical regions like primary and secondary somatosensory cortex, insular cortex and anterior cingulate cortex and amygdala.

Primary somatosensory cortex region is associated with the sensory or discriminative aspects and the secondary somatosensory cortex is associated with additional affective or cognitive functions. Amygdala, on the other hand, is known to be associated with conscious awareness and cognitive evaluation of pain. Furthermore, the basal ganglia, cerebellum, amygdala, hippocampus and some regions of the temporal and parietal cortices have been discussed as belonging to the “extended pain matrix” [12]. In this study, pre-frontal cortex has been chosen as the area of study because it lies in the superficial layers of the brain and hence, can be easily measured and also, pre-frontal cortex has been reported to be responsible for pain perceptions [10].

2.5 Pre-frontal Cortex:

The prefrontal cortex (PFC) is located in the very front of the brain, just behind the forehead. The Brodmann areas 9, 10, 11, 12, 46, and 47 are a part of the pre-frontal cortex.

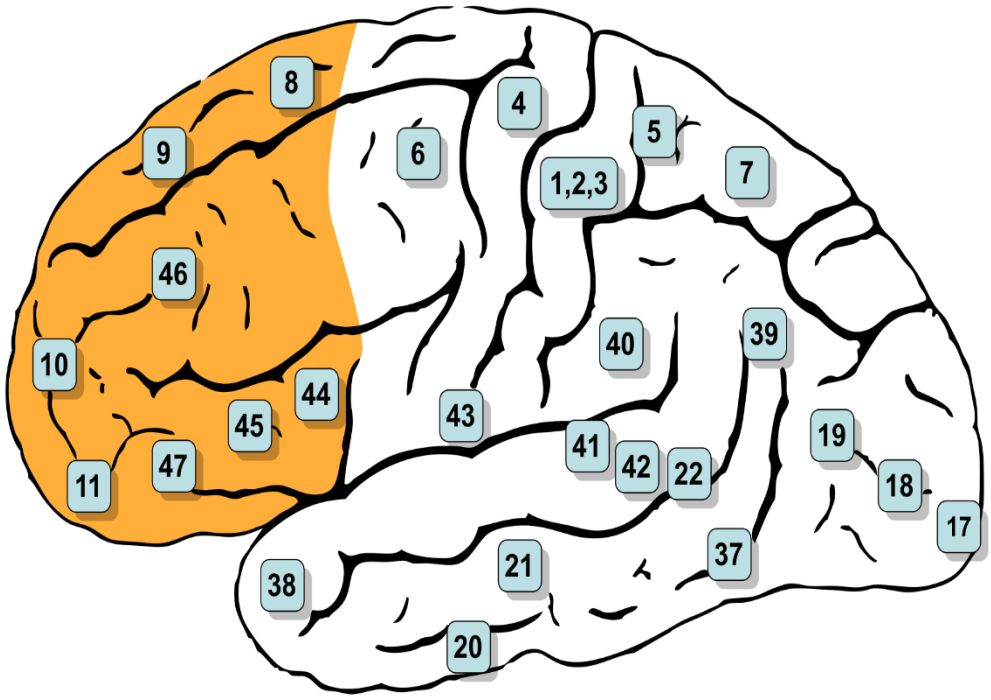

Figure 2.2 shows the representation of The Brodmann areas 9, 10, 11, 12,44, 46, and 47 in the pre-frontal cortex

[https://en.wikipedia.org/wiki/Prefrontal_cortex]

This region is responsible for cognitive control, complex behavior, planning and decision making. One of the most important function of the pre frontal cortex includes the to abilities to differentiate among conflicting thoughts, determine good and bad, better and best, same and different, future consequences of current activities, working toward a defined goal, prediction of outcomes, expectation based on actions, and social "control". This is termed as executive function.

2.6 Pain Habituation

According to the 'Dual process theory' proposed by Groves and Thompson, sensitization and habituation are two separate opposing processes. These processes play a very

important role in the final outcome of painfulness of repeated exposure to painful stimuli [14]. Sensitization occurs after repeated or intense painful stimuli after it crosses the limit of activation and its response to painful stimulation inputs are amplified. Habituation is described as a decrease in pain and pain related responses with continuous or repetitive pain stimulation.

Chapter 3

Instrumentation and Data acquisition

3.1 Materials and methods:

10 healthy subjects from different departments aged between 22 – 35 years in the University of Texas at Arlington volunteered for the FNIRS measurements. All the subjects were right dominant and they were asked if they had any history of neurological disorders and if they were under medications during the day of the experiment. Subjects were slightly bald near in the prefrontal cortex area of the head so that there was less interference of hair for proper placement of probes. Written consent was obtained from all the subjects before the measurement. The protocol used in the study was approved by the Institutional Review Board of UTA.

3.2 Instruments

3.2.1 FNIRS Imaging System (Cephalogics)

Cephalogics FNIRS imaging system, a multi-channel, continuous wave imaging technology was used for measuring the signals from the neuronal activity. The system consisted of and frequency-encoded lasers and an array of avalanche photo-diodes (APDs) acting as sources and detectors, a DSP control board for data acquisition and a computer. The instrument consisted of multiple sources that comprised of three 750-nm and one 830-nm light emitting diodes each and multiple detectors that were connected to avalanche photodiodes. The head optode array used in this study consisted of 80 sources and 80 detector channels that included 16 short separation sources and detectors. A real-time Digital Signal Processing (DSP) based control card in the system allows real time demodulation of signals. Thus, it makes the set-up more reliable, faster and easier as well as reduces the computing time for post-processing.

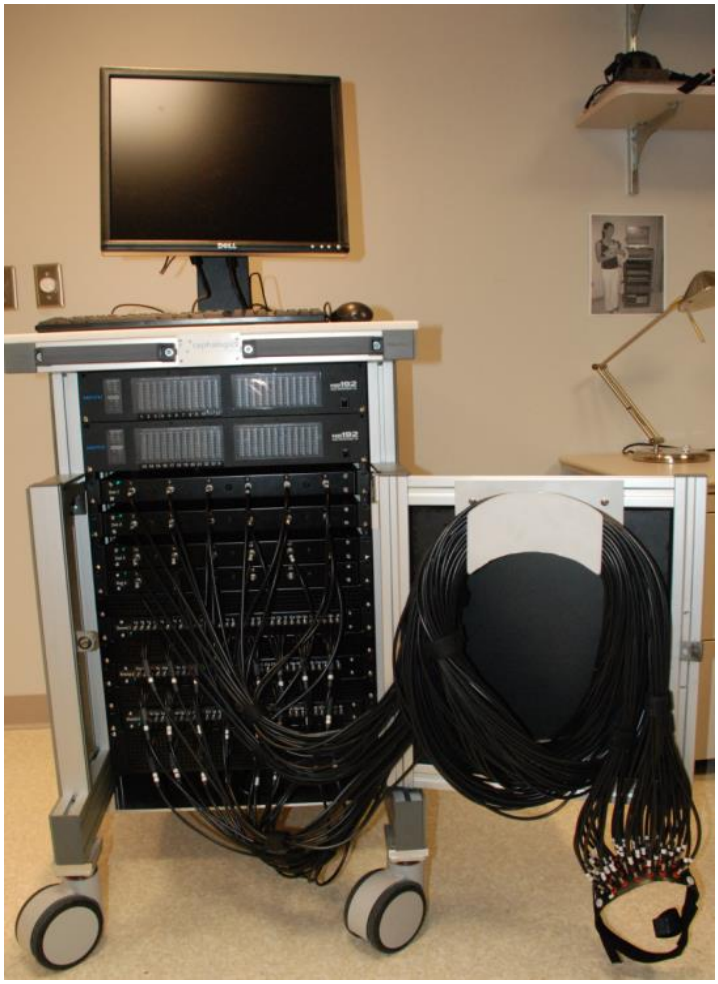

Figure 3.1 shows the experimental setup of CEPHALOGICS FNIRS Imaging system

3.2.2 Thermal pain stimulation device

The PATHWAY Pain & Sensory Evaluation System (Medoc) was used which can generate a wide range of temperatures, 41-47°C in our case, in order to evoke various levels of innocuous and noxious pains an advanced, computerized thermal stimulator, designed for advanced neurological and pain research.

The system consists of ATS thermode that are attached to the skin of the tested subject to obtain contact thermal stimulation.

The PATHWAY system offers designated software, for easy control and management of the system. PATHWAY software can be controlled by other research programs such as “LabView” and “MATLAB, for activating stimulation protocols, using analog and I/O channels.

Figure 3.2 shows the experimental set up of the PATHWAY thermal stimulator machine

3.2.3 Easy topo Digitizer:

Mapping of optode position information on the brain is obtained using a 3D digitizer Patriot Digitizer, Polhemus Inc). it is a light, compact, inexpensive electromagnetic digitizer system that helps localize the electrode placement and head landmarks by NIRS system.

Figure 3.3 shows the experimental set up of the PATRIOT digitizer machine

A locator software is used to control the measurements that obtains the data and outputs a 3D position measurements for electrodes, fiducial marks and other points of the head. Unlike other conventional digitizer machines, there is no necessity of maintaining a clear line-of-sight between receiver and transmitter.

Limitations faced by the conventional machines such as signal blocking and interference from sonic and laser devices have been solved in this technology. The main components of the 3D digitizer system include: electronic unit, transmitter, receiver and a stylus.

Electronics Unit comprises of the hardware and software units that generate and sense the magnetic fields, compute position and orientation, and interface with the host computer via an RS-232. The transmitter acts as a reference frame for the measurements. The transmitter and receiver, both comprise of electromagnetic coils in a plastic shell that transmit and receive magnetic fields. The stylus pen is used for digitizing the electrode locations and selecting the contours on a subject's head.

3.3 Experimental Protocol:

A short pre-experimental paradigm is conducted on the subject to estimate the perception of pain. The thermode 16*16 mm2 from the ATS thermal stimulator is attached to the patient's dominant arm. The temperature was increased from 41°C to 47°C using the staircase approximation method. Each subject was asked to rate the perception of pain on the scale of 0-10 by using the visual analog pain rating. The perception rating levels are 0,3,5 and 7 for no pain, low pain, moderate pain and high pain. The highest pain temperature that was rated as 7 was selected in the actual experiment.

After estimating the pain perception, the subject was asked to relax comfortably on a chair and a measuring tape was used to measure the size of the head. Nasion(Nz), inion (Iz), left ear , right ear were marked representing the 10-20 international system of electrode placement. The pre-frontal area of the brain was estimated approximately and the probe was attached to the subject's head and held firm using a Velcro and elastic bandage strap. The distance between the Nz and the first row of the strap was measured for each subject to ensure that the placement was accurate across everyone. The probes were covered using an elastic bandage to block the ambient light. The hair covering the subject's forehead scalp area was brushed aside before placing the probe on the subject's forehead. After placing the probe on the subject's forehead, remaining strands of hair, if any, blocking the optodes were brushed aside to obtain cleaner signals. The

subject was asked to place the dominant arm comfortably. The thermode was attached to the subject's dominant arm. The subject was asked to avoid head and body movement. The room lights were turned off after the entire set up.

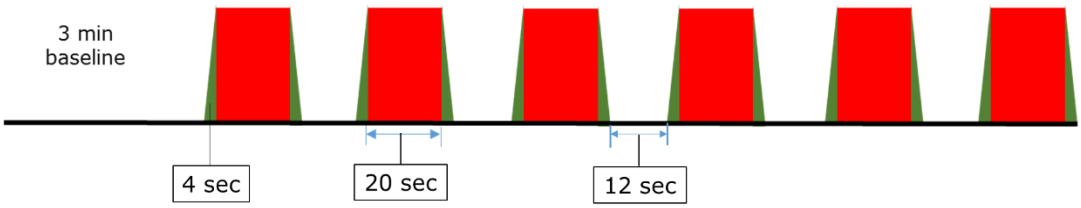

Figure 3.4 Experimental protocol

The protocol comprised of initial three minutes of baseline measurements followed by six blocks with 28 seconds of pain stimulation followed by approximately 12 seconds of recovery period. The experiment lasted for about 10 minutes. After the experiment, the digitizer measurements were obtained for recording the neuro-anatomical position of the optodes. Nasion(Nz), inion (Iz), left ear , right ear and the central point between Nz-In and AL-AR was measured using a 3D digitizer. Then using NIRS-SPM, a freely downloadable Matlab-based software package from http://bisp/kaist.ac.kr/NIRS-SPM [24,25], the representation of spatial location of optodes on a human brain template were obtained.

3.4 Probe Geometry:

The configuration of the probe geometry used in this study is as shown in the figure. 20 sources and 20 detectors were used in this study. The distance between each row was around 2.5 cm and the source to detector distance perpendicular to each other was 3cm, the source to detector distance diagonal to each other was 3.9cm. The total area covered by this probe geometry was 180cm.

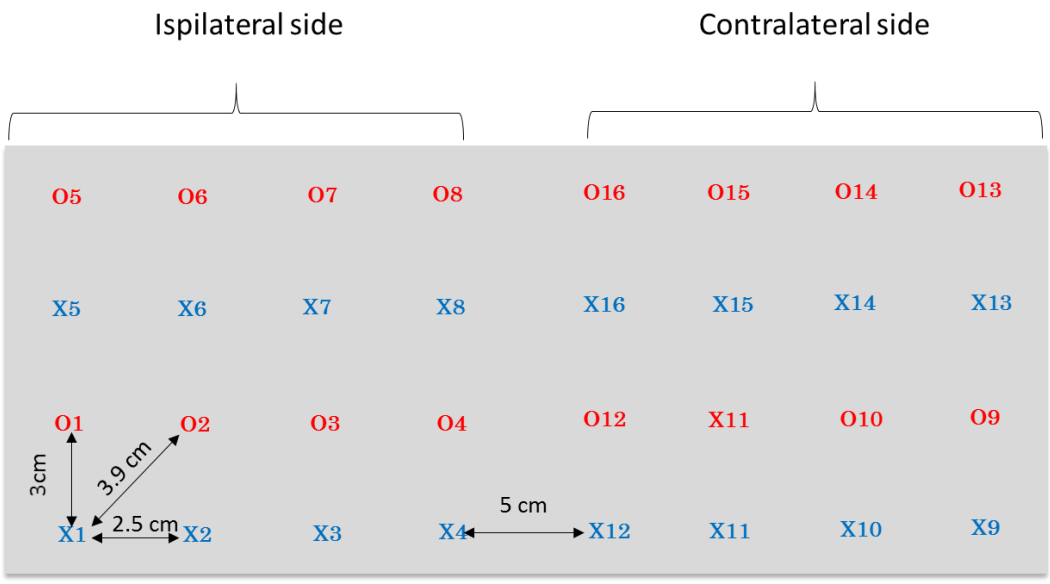

Figure 3.5 shows the configuration of the probe geometry used in this study

3.5 Data processing

The raw data from the FNIRS machine was converted into NIRS file using a Matlab based software from http://www.nmr.mgh.harvard.edu/DOT/resources/homer/forum.html. This software is extensively used for the pre-processing of the signals from the brain. For getting rid of the respiratory noise and heart rate interference, the data is filtered using high pass and low pass filter. High pass frequency of 0.01Hz and low pass frequency of 0.1 Hz is used not only to avoid physiological interference, but also to avoid instrumental noise due to the high sampling rate of the instrument. The stimulus timing information of 180, 245,295, 345, 395 455 seconds was entered in order to perform block averaging of the signal. This block averaged data of 50 seconds was extracted and stored in the computer for all the 80 channels for further processing.

Chapter 4

Results & Discussion

4.1 Experimental Results:

After importing the data for all the channels from HOMer, the latter half of the processing was done in MATLAB. Since the HbO signal in the HOMer correlate to the BOLD signals in the Functional Magnetic Resonance Imaging (FMRI), HbO signals have been studied further in this experiment. The raw optical intensities from all the channels were checked individually for each subject in order to identify any channels with large noise.

4.1.1 Hemodynamic changes due to painful stimuli (PART 1)

The painful stimuli and the post stimulus resting state duration were compared using the block averaged HbO signals across all the 8 subjects. The block averaged data of the initial stimulus interval of 28 seconds for each subject was saved from the HOMer. Similarly, the block averaged data for the post stimulus interval of 28-50 seconds was also saved for each subject. Using MATLAB, the data points of each channel was averaged across all the 8 subjects.

4.1.1.1 Cluster based approach:

A cluster based approach was used to group the channels of each tiny area. Eighteen different clusters were formed in this study to cover the whole measured area comprising of the pre-frontal cortex. Each cluster consisted of 2 to 6 channels. For group-level cluster analyses, the temporal profiles of all the channels in each cluster were averaged first for

each subject, and then further averaged across all eight subjects.

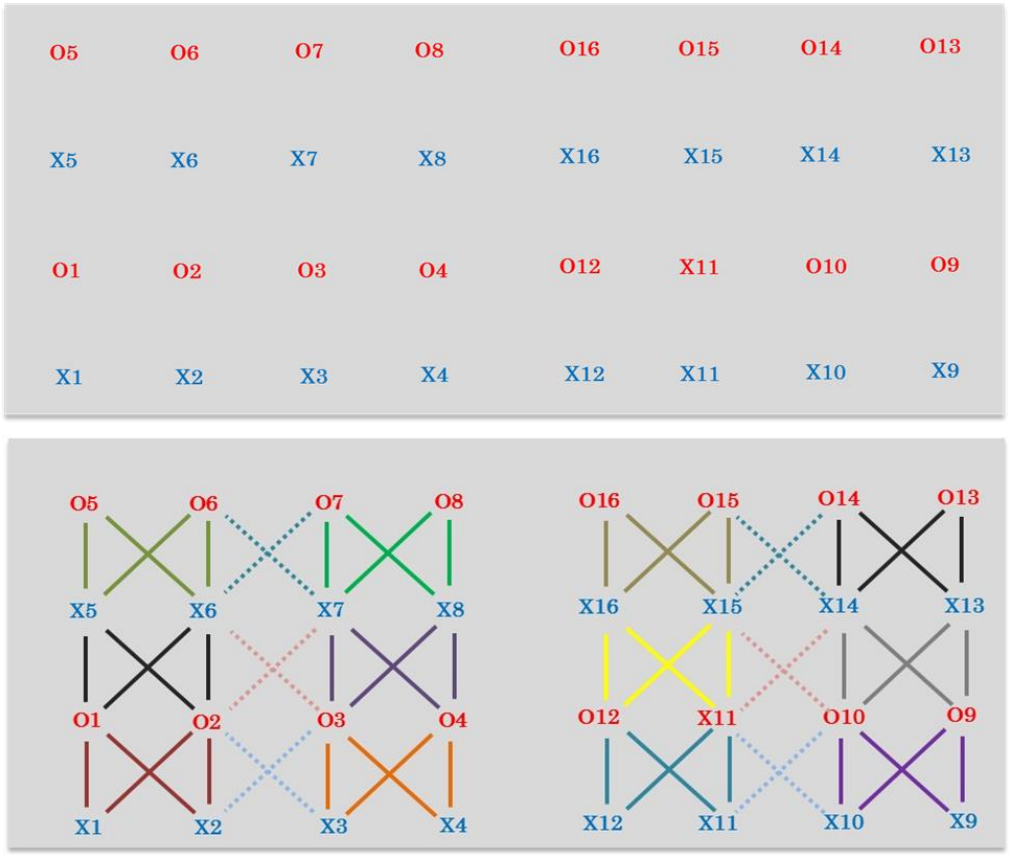

Figure 4.1 shows the 18 clusters formed on the ispilateral and contralateral side of the brain.

The grand-averaged temporal profiles of HbO signals for all the clusters are labeled as C1, C2,..,.., and C18, as shown in Figure, in response to both stimulus interval (0-28 seconds) and post-stimulus interval (28-50 seconds). Clusters C1, C2,C3,C4,C5,C6,C7,C8 and C9 are on the ipsi-lateral (right) side of the pre-frontal lobe with respect to the stimulation side; C10,C11,C12,C13,C14,C15,C16,C17 and C18 are on the contralateral (left) side.

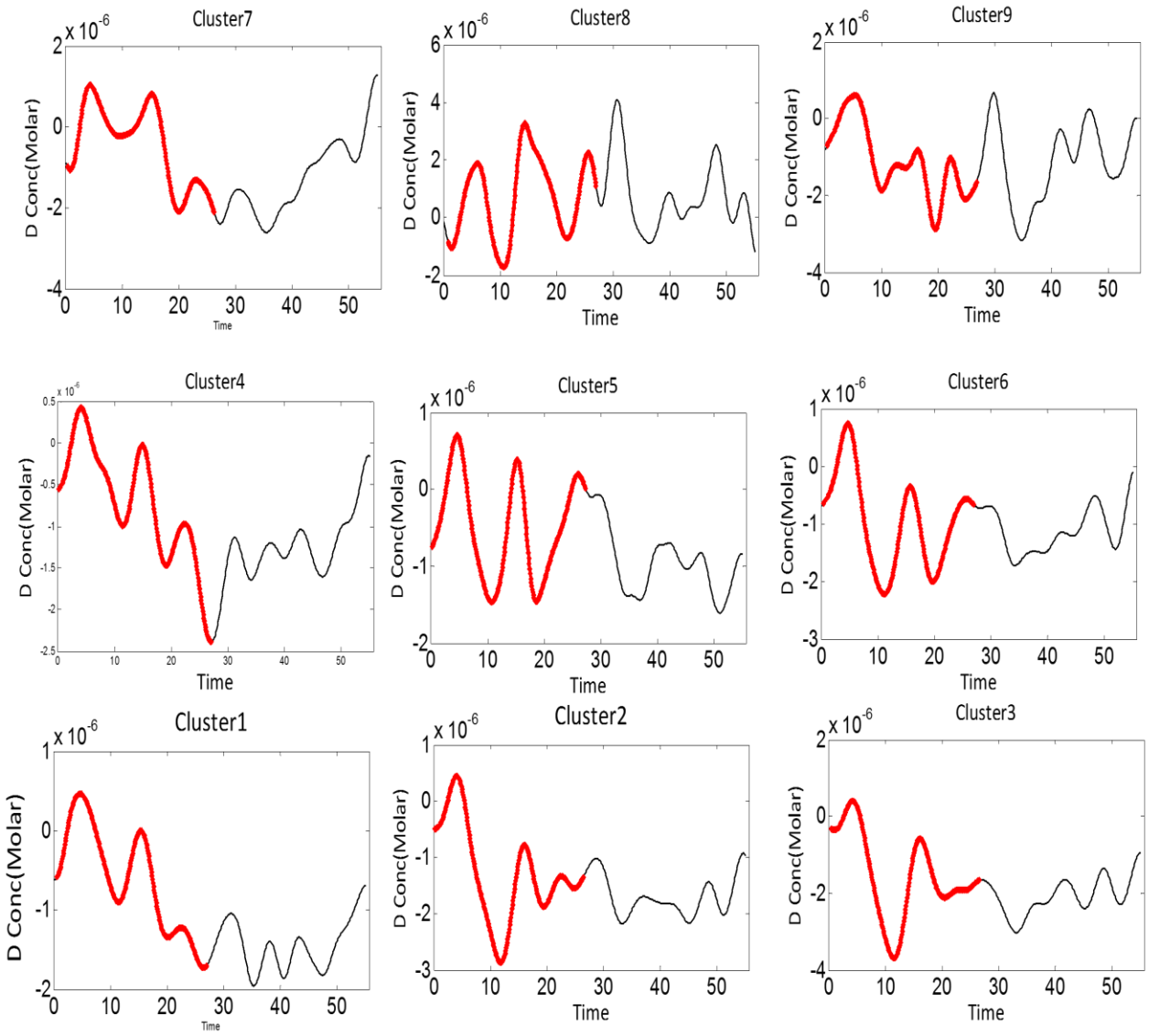

Figure 4.2 represents the clusters (0-9) on the ispilateral side of the brain with comparison of the temporal profiles of the stimulus interval and post stimulus interval.

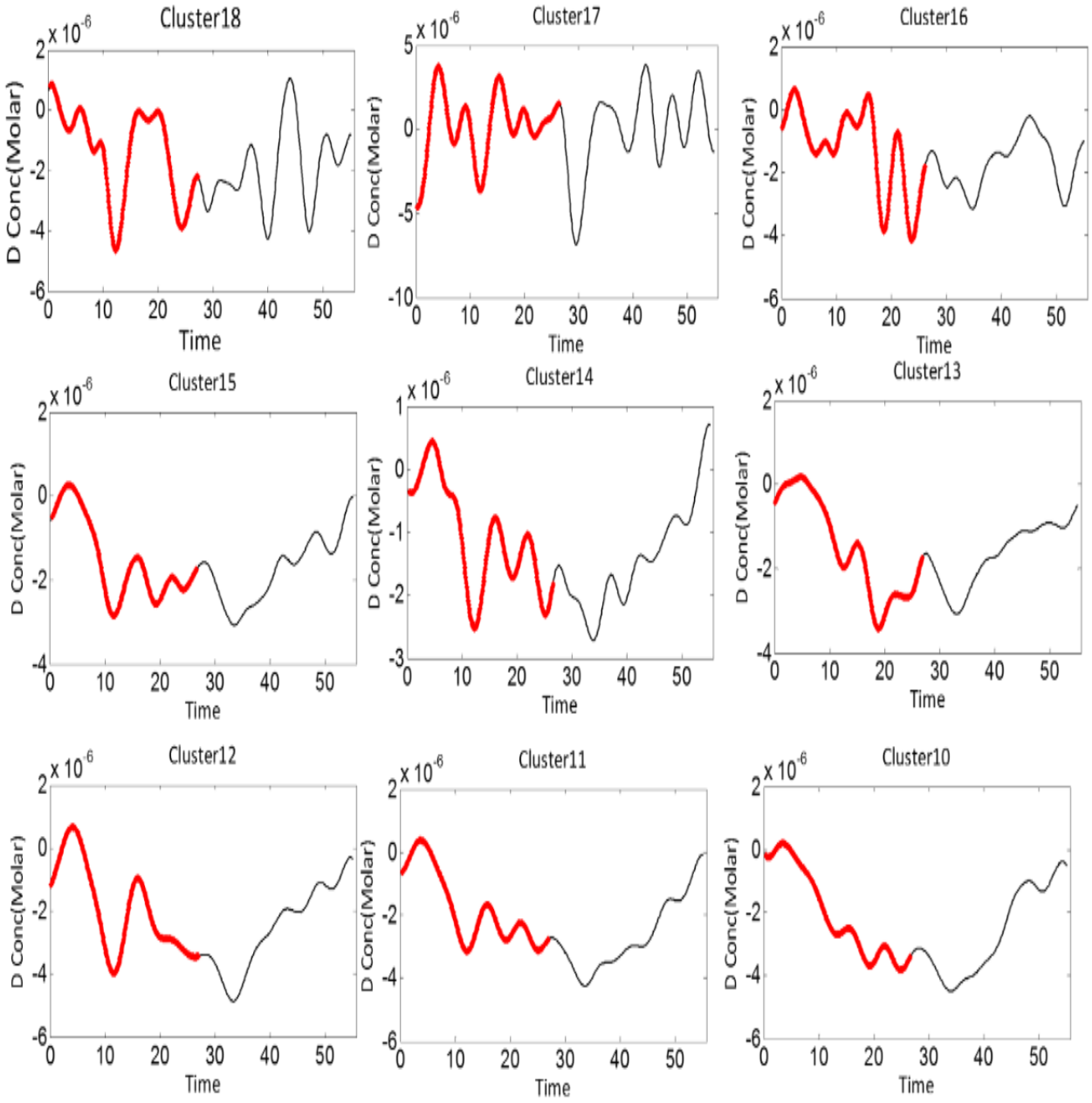

Figure 4.3 represents the clusters (10-18) on the contralateral side of the brain with comparison of the temporal profiles of the stimulus interval and post stimulus interval.

4.1.1.2 Statistical Analysis:

Since it is difficult to conclude whether these clusters actually show any significant hemodynamic changes from the above graphs, we performed statistical analysis on each individual 64 channels to see if any of these channels show significant difference. The block averaged data for the stimulus interval (0-28 seconds) and the post stimulus interval (28 – 50 seconds) is saved in Microsoft Excel to perform statistical analysis. The data points of each of these channels for both the intervals were averaged for one subject. Later, comparison of the stimulus interval data and the post stimulus interval data was performed for each channel to see if there was any significant difference between them. This statistical comparison was performed by using one sample t-test against the hypothetical mean value of 0.

4.1.1.2.1 Stimulus interval (0-28 seconds):

13 out of the 60 channels showed significant difference with p values < 0.05. By using this restrictive threshold of 0.05, we can identify a few active channels but at the same time we might risk a few channels that are truly active due to their lower significant values. This might lead to increase in the Type II errors which leads to removal of functionally significant channels. To avoid this, False Discovery Rate (FDS) approach is used which describes the proportion of positive results that are actually false positives. FDR is a less stringent correction done to see if there are many activated channels compared to Family-wise Error Rate (FWER).

FDR corrections involves a few important steps. First, all the p values are arranged in the order from the smallest value to the largest value.

Table 4.1 represents the p-values of the channels that shows significant hemodynamic changes during the stimulus interval (0-28 seconds)

Channel No	P-value (one tailed	Area covered
55	0.0021	Dorsolateral Prefrontal Cortex (BA 9)
26	0.0058	Dorsolateral Prefrontal Cortex (BA 9)
23	0.0097	Dorsolateral prefrontal cortex (BA 9 and 46)
51	0.0191	Dorsolateral prefrontal Cortex (BA46)
58	0.0217	Dorsolateral Prefrontal Cortex (BA 9)
35	0.0252	Dorsolateral prefrontal Cortex (BA46)
25	0.0346	Dorsolateral Prefrontal Cortex (BA 9)
5	0.0404	Dorsolateral prefrontal Cortex (BA46)
53	0.0439	Dorsolateral Prefrontal Cortex (BA 9)
28	0.0464	Dorsolateral prefrontal cortex (BA 9 and 46)
9	0.0479	Frontopolar area (BA 10)
40	0.0283	Frontopolar area (BA 10)
30	0.0445	Dorsolateral Prefrontal Cortex (BA 9)

An algorithm is used that identifies the channel with p value (Pi) greater than channels ranking in the list (i) divided by total no. of channels as corrected by desired FDR (q). All the channels that range from P1 to Pi are marked as significant.

$$Pi \leq \frac{iq}{C}$$

Pi – p value desired

i – No. of channels ranking in the list.

q – p value considered

C – total no.of channels

In our case, the values of i, q and C are 13, 0.05 and 60.

$$Pi \leq 13 \times \frac{0.05}{60}$$

Thus, the desired p value was calculated to be less than 0.0108. And so, there were only three channels with values less than 0.0108.

Table 4.2 represents the p-values of the channels that shows significant hemodynamic changes during the stimulus interval (0-28 seconds) using False Discovery Rate

Channel No	P-value (one tailed	Area covered
55	**0.0021**	**Dorsolateral Prefrontal Cortex (BA 9)**
26	**0.0058**	**Dorsolateral Prefrontal Cortex (BA 9)**
23	**0.0097**	**Dorsolateral prefrontal cortex (BA 9 and 46)**

4.1.1.2.2 Recovery period (28-50 seconds)

13 out of the 60 channels showed significant difference with p values < 0.05. False discovery corrections were done for avoiding Type II errors. So, the similar calculations were performed for the recovery period of 28-50 seconds. All the p values

are arranged in the order from the smallest value to the largest value. The Pi was calculated which was found to be less than or equal to 0.0108.

Table 4.3 represents the p-values of the channels that shows significant hemodynamic changes during recovery period (28-50 seconds)

Channel no	P-value (one tailed)	Area covered
55	0.0064	Dorsolateral Prefrontal Cortex (BA 9)
26	0.0191	Dorsolateral Prefrontal Cortex (BA 9)
30	0.0268	Dorsolateral Prefrontal Cortex (BA 9)
8	0.0275	Frontopolar area (BA 10)
36	0.0326	Dorsolateral prefrontal Cortex (BA46)
58	0.0337	Dorsolateral Prefrontal Cortex (BA 9)
40	0.0362	Frontopolar area (BA 10)
53	0.0386	Dorsolateral Prefrontal Cortex (BA 9)
49	0.0433	Dorsolateral Prefrontal Cortex (BA 9)
60	0.0234	Dorsolateral Prefrontal Cortex (BA 9)
51	0.0244	Dorsolateral prefrontal Cortex (BA46)
54	0.0317	Dorsolateral Prefrontal Cortex (BA 9)
43	0.0323	Pars opercularis, part of Broca's area (BA44)

Out of the 10 channels, only 1 channel showed p values less than 0.01 and were found to be significant.

Table 4.4 represents the p-values of the channels that shows significant hemodynamic changes during the recovery period (28-50 seconds) using False Discovery rate

Channel no	P-value (one tailed)	Area covered
55	**0.0064**	**Dorsolateral Prefrontal Cortex (BA 9)**

4.1.1.3 Brain mapping:

At the same time, t-stat value for each of these channels were also calculated for both stimulus interval (0-28 seconds) and recovery period (28-50 seconds). Binary code 1 was put across all the channels that had p values less than 0.01 which showed significant difference between them. Similarly, a binary code of 0 was put across all the channels which showed a p-value more than 0.0108. This was done for both the data sets i.e. stimulus interval of 0-28 seconds and post stimulus interval of 28-50 seconds.

To visualize the difference between the stimulus interval and the post stimulus interval activation, these p values and the t-stat values of the one sample t test were mapped on the human brain using 3D digitizer Patriot Digitizer measurements. First, the numbering of the sources and detectors were arranged according to the order of the co-ordinates measured using the stylus marker to make sure that the order of the co-ordinates measured coincided with the numbering of sources and detectors. Each point of the digitizer measurement consisted of two rows of data with six readings each. The last three numbers of both the rows were deleted since only the x, y and z co-ordinates were used for further calculations. Now, the row 1 was deleted from the row 2 set of co-ordinates to calculate the final x, y, z co-ordinates of each digitizer point measured. Now for calculating the location of each of the 60 channels each channel was defined with its source and detector combination starting from Channel 1 (Source 1, Detector 1) to

channel 60 (Source 20, Detector 20). After defining each channel with its sources and detectors and their respective co-ordinates, an average of each co-ordinate was calculated. For example, for Channel 1, source 1 is defined as x1, y1, z1 and detector 1 is defined as x2, y2, z2. Channel 1 will be calculated as ($\frac{x1+x2}{2}$, $\frac{y1+y2}{2}$, $\frac{z1+z2}{2}$). All the channels that created a boundary on the ispi lateral and contralateral side of the probe geometry were copied separately. All these files along with the p value & t-stat value files were uploaded in the Brain mapping software and the channels and the p value activations were mapped on the brain.

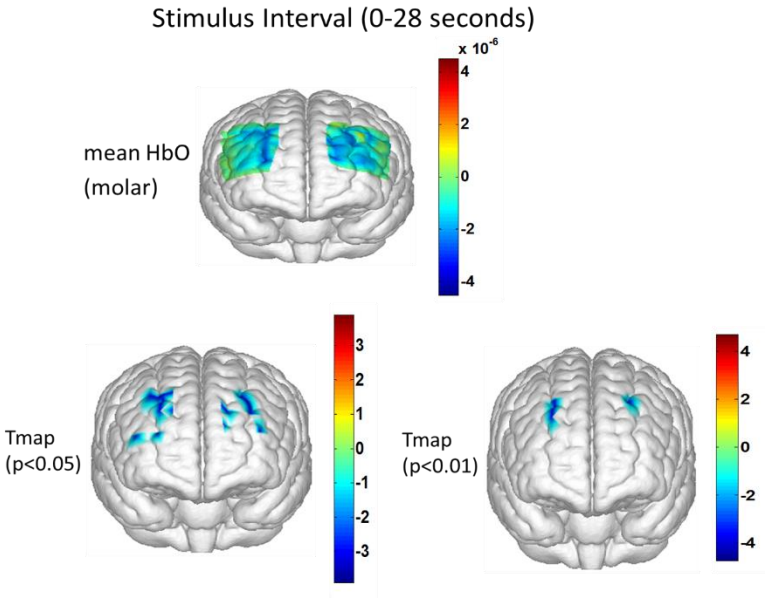

Figure 4.4 shows Brain mapping of Mean HbO (molar), Tmaps of p<0.05 (Two sample t test) and p<0.0108 (FDR) during the stimulus Interval

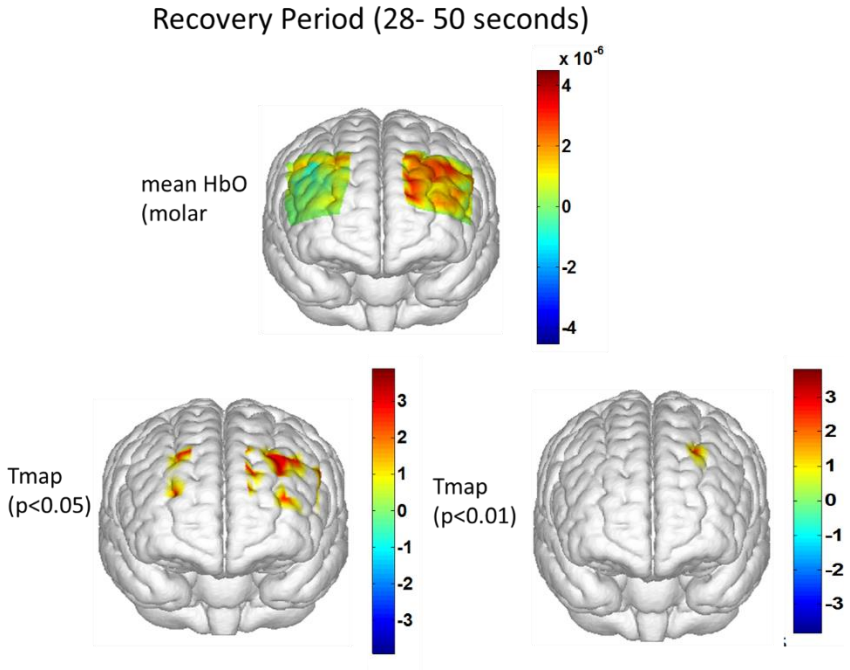

Figure 4.5 shows Brain mapping of Mean HbO (molar), Tmaps of p<0.05 (Two sample t test) and p<0.0108 (FDR) during the recovery period

From the figures representing the activations and deactivations, from the stimulus interval duration, dorsolateral prefrontal cortex, frontopolar area and pars triangularis Broca's area, showed deactivation signals from the 60 channels.

In the post stimulus interval durations, activations were observed in the dorsolateral prefrontal cortex, small parts of broca area, pars triangularis Broca's area, and the frontopolar area from the 60 channels.

4.1.2 PART 2 (Pain habituation):

In this study, we hypothesized that pain habituation exists and that giving repetitive thermal stimuli causes reduced activations or reduced deactivations of the signal with

respect to time. To see the pain habituation effects in the last 2 blocks of the experimental protocol, we compared the first 2 and the last 2 blocks by performing statistical analysis.

4.1.2.1 Statistical Analysis:

4.1.2.1.1 Stimulus interval (0-28 seconds)

The painful stimulus duration (0-28 seconds) were compared for the first 2 blocks and the last 2 blocks using the block averaged HbO signals across all the 8 subjects. To calculate if there was any significant difference between the stimulus interval of 0-28 seconds between the first 2 blocks and the last 2 blocks, the data was saved in Microsoft excel sheet by importing the block averaged data for each subject from HOMer. All the data points were averaged across channels for each subject. By using two sample paired t test for equal variance, the p values were calculated to see if there was any significant difference between the first 2 blocks and the last 2 blocks for any of the 60 channels. It was seen that there was no significant difference between the first 2 blocks and last 2 blocks for 0-28 seconds in any of the 60 channels.

Since 28 second duration was a very long duration to find any significant pain habituation effects, we chose to split the 28 second duration into three small sets of duration and further analyze these small durations for any significant pain habituation effects. The 28 second duration was split into initial phase (0-10 seconds), middle phase (10-20 seconds) and later phase (20-28 seconds).

4.1.2.1.2 Initial Phase (0-10 seconds):

To calculate if there was any significant difference in the 0-10 seconds duration between the first two blocks and the last two blocks to see pain habituation effects, two sample t test with equal variance was used. The p-values for all the 60 channels were found to be greater than 0.05 and so we could conclude that none of the 60 channels showed pain habituation effects between the first 2 blocks and the last 2 blocks.

4.1.2.1.3 Middle phase (10-20 seconds):

To calculate if there was any significant difference in the 10-20 seconds duration between the first two blocks and the last two blocks to see pain habituation effects, two sample t test with equal variance was used. The p-values Channel 48 was found to be less than 0.05 and so we could conclude that Channel 48 out of all the 60 channels showed pain habituation effects.

4.1.2.1.4 Last phase (20-28 seconds):

To calculate if there was any significant difference in the 20-28 seconds duration between the first two blocks and the last two blocks, two sample t test with equal variance was used. 10 out of the 60 channels showed p values less than 0.05 and they showed pain habituation effects.

Table 4.5 represents the p values of the channels that showed significant difference between the first 2 blocks and the last 2 blocks.

Channel No	P-value (one tailed)	Area covered
10	0.035078647	Frontopolar Area (BA 10)
22	0.036198322	Dorsolateral Prefrontal area (BA 46)
35	0.045280084	Dorsolateral Prefrontal area (BA 46)
37	0.045969615	Frontopolar Area (BA 10)
38	0.04669726	Frontopolar Area (BA 10)
40	0.011950404	Frontopolar Area (BA 10)
46	0.019032005	Dorsolateral Prefrontal area (BA 46)
47	0.015892317	Dorsolateral Prefrontal area (BA 46)
51	0.023899198	Dorsolateral Prefrontal area (BA 46)
52	0.022059174	Dorsolateral Prefrontal area (BA 9& 46)

For better understanding, bar graphs were plotted to compare the difference between the firs 2 blocks and the last 2 blocks. Error bars were plotted on each individual channel to check for errors or uncertainty.

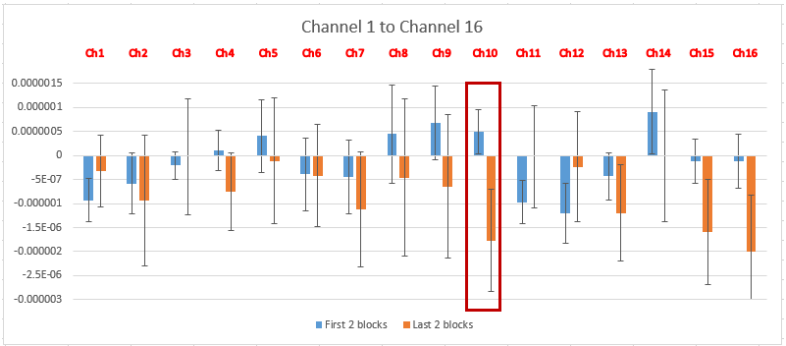

Figure 4.6 The bar graphs plotted to show comparison of hemodynamic changes First 2 blocks and Last 2 Blocks (Channels 1-16). The red highlighted bars show the channel 10 which had p-value less than 0.05

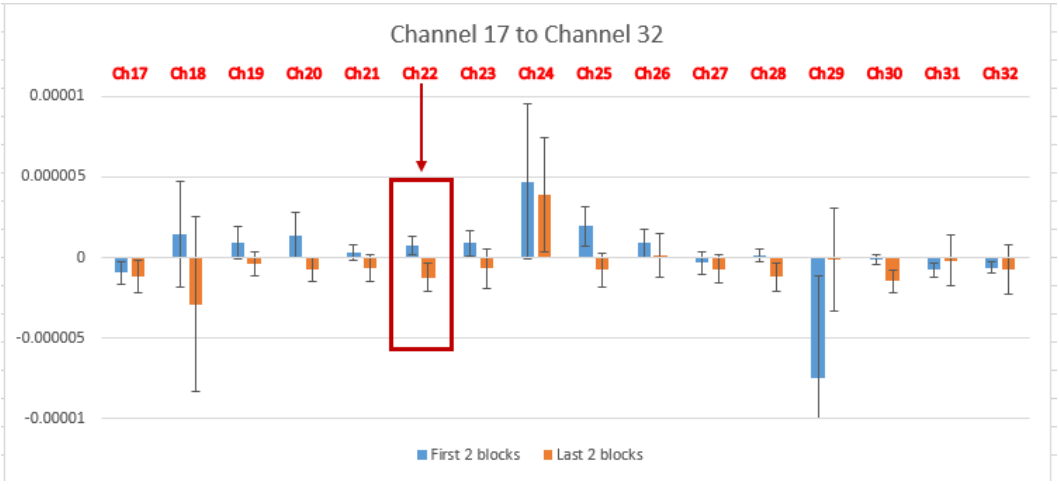

Figure 4.7 The bar graphs plotted to show comparison of hemodynamic changes First 2 Blocks and Last 2 Blocks (Channels 17-32). The red highlighted bars show the channel 10 which had p-value less than 0.05

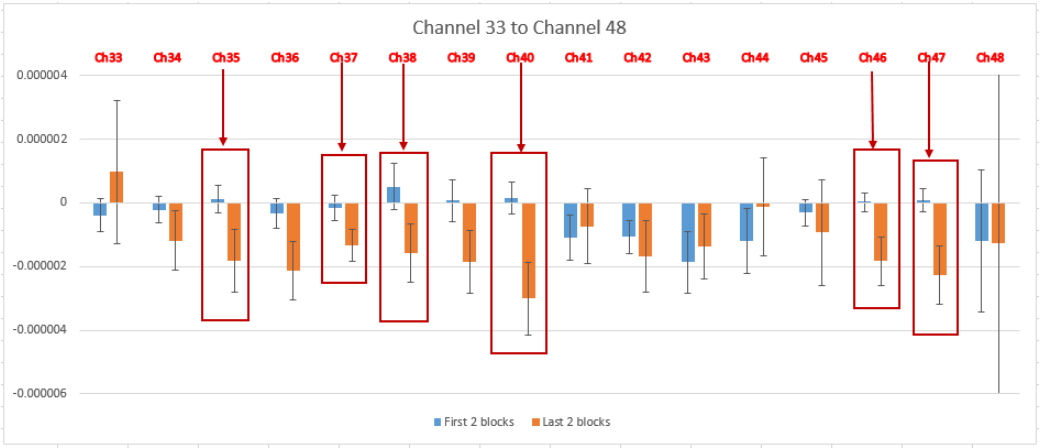

Figure 4.8 The bar graphs plotted to show comparison of hemodynamic changes First 2 Blocks and Last 2 Blocks (Channels 33 to 48). The red highlighted bars had p values less than 0.05

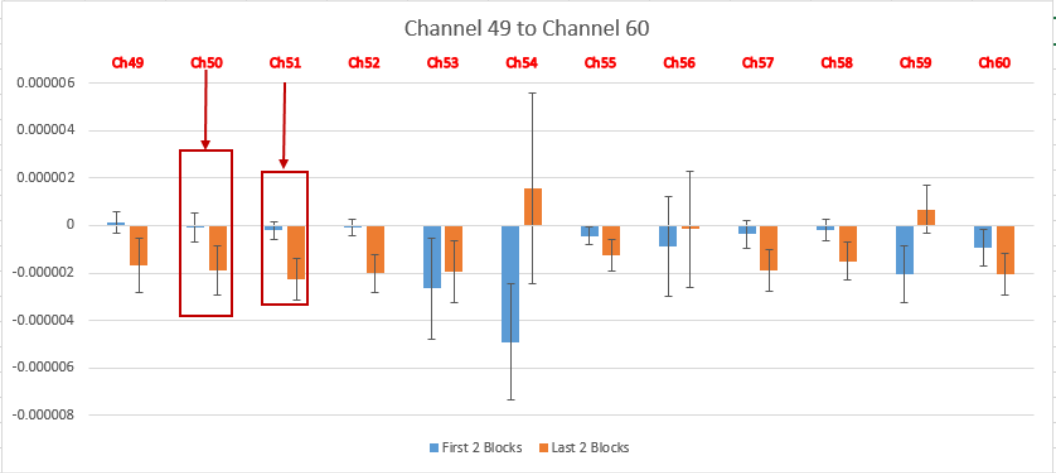

Figure 4.9 The bar graphs plotted to show comparison of hemodynamic changes First 2 Blocks and Last 2 Blocks from channels 49 to 60. The red highlighted bars show bars had p values less than 0.05

4.1.2.2 Brain mapping:

To avoid the risk of the increase in Type II errors due to the restrictive threshold of 0.05, FDR was used. . All the p values are arranged in the order from the smallest value to the largest value. The Pi was calculated which was found to be less than or equal to 0.00833. Out of the 10 channels showing pain habituation. None of those channels had p-values less than 0.008.

Therefore, brain mapping was performed for channels that showed significant differences using Two Sample t test. The averaged HbO values across all 8 subjects for the first 2 blocks and the last 2 blocks were calculated for 60 channels individually. The Averaged HbO values of the last 2 blocks were subtracted from First 2 blocks and ΔHbO values were plotted on the brain mapping software. Apart from this, t stat values were calculated for each of these 60 channels. The t stat values of the channels having p-values less than 0.05 were also plotted on the brain mapping software.

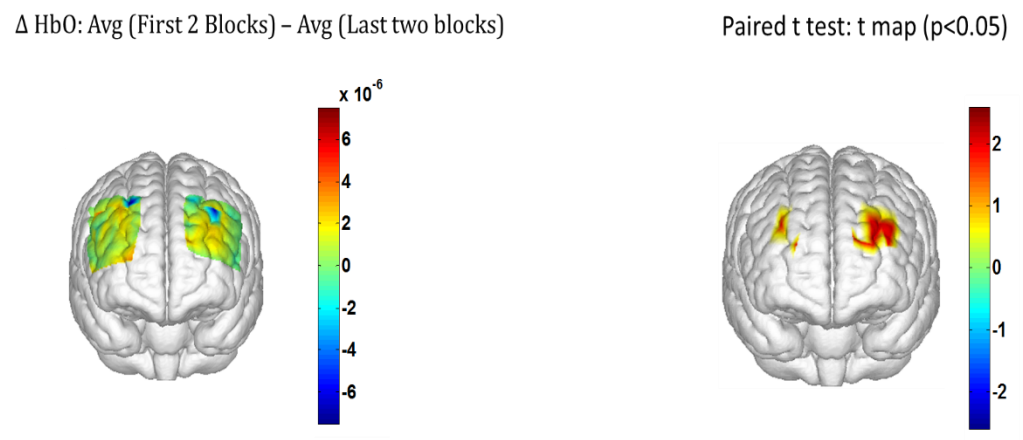

Figure 4.10 shows the brain mapping of ΔHbO and t stat values with p values < 0.05

Pain Habituation effects were found in the areas of Dorsolateral PFC (BA 9 and 46) and fronto polar Cortex (BA 10) majorly. Also it was observed that more habituation was found on the contralateral side of PFC.

4.2 Discussion:

A non-invasive FNIRS technique was used to assess a hemodynamic activity in response to thermal pain stimuli. The data analysis was divided into two main parts. The PART 1 analysis was done to see if there were any activations or deactivations observed in the entire prefrontal cortex area of the brain during the pain stimulation as well as post stimulus interval. From this study, we observed that there were deactivations found in the brain during the stimulus interval from both long and short separation channels. Deactivations were found in dorsolateral prefrontal cortex (BA 46 and BA9), frontopolar area (BA10) from 60 channels. In most of the pain research studies conducted so far, pain activations have been properly explained and interpreted compared to pain

deactivations. Decrease in the hemodynamic activity of the brain during pain have been briefly reported or left undiscussed.

These results were consistent with a few similar studies done previously. Recent fMRI reports have also shown negative BOLD response under mechanical (Lui, et al., 2008) and thermal stimulation (Kong, et al., 2010; Moulton, et al., 2006) in the pre-frontal cortex area. In a neuroimaging study conducted on pain by Harvard Medical School and the Dept. of Psychiatry, two different pain levels(low pain and high pain) were administered to the subjects and their hemodynamic activity of the brain was observed using FMRI. Deactivations were found in the anterior cingulate cortex, occipital/middle temporal gyrus, precuneus, midcingular and posterior cingulate cortex, motor/premotor cortex, hypothalamus, and cerebellum during the low pain stimulation. Deactivations were also found in the bilateral medial prefrontal cortex, anterior cingulate cortex, posterior cingulate cortex, precuneus, and lateral occipital gyrus S1/M1, etc. Since, negative BOLD responses showed correlations with the decreased neuronal activity, the results implied that large no. of the pain matrix show deactivations during pain. These signals deactivations were shown widely in the 'default mode network' areas such as bilateral MPFC, posterior cingulate cortex, precuneus, hippocampus, and lateral temporal cortex. Since default mode network is that area of the brain that shows activations when human brain is left to think to itself undisturbed, it is known to show deactivations during goal oriented behaviors. In this study, we can hypothesize that since pain intensity during the thermal stimulation can pose as a threat to the subject, they tend to divert their attention to explore alternative scenarios to escape the fear of harm caused by pain. This thought of diversion will act against the DMN inhibition (a feeling that makes one self-conscious and act natural) due to the painful stimuli [17]. Apart from this, it has been said that activations and deactivations during the pain stimulus might underlie different

aspects of pain experience [17]. Other possible explanations for deactivations could possibly be invoked by pain induced synaptic inhibition and vasoconstriction (Devor, et al., 2007) [18]. In a study conducted by W G Derbyshire and his colleagues, six female chronic patients suffering from atypical facial pain were induced with thermal stimuli in the right hand and their hemodynamic changes were observed using a PET scanner. Increased CBF was found in the amygdala and decreased CBF was found in the PFC [23].

On the other hand, it was also found that during the post- stimulus interval, activations were found in the dorsolateral prefrontal cortex from the 60 channels. In the post stimulus interval, the subject was asked to sit idle and passive for approximately 12-17 seconds until the next pain stimuli was induced. During this interval duration, the subjects were left undirected to think and the default mode networks were found to be active in the prefrontal cortex region of the brain.

Pain is modulated in the prefrontal cortex because it receives sensory input from the limbic system and shares a relationship with the motor cortex, such that based on the intensity of pain perceived, the prefrontal cortex communicates to other tissues to respond accordingly [19]. In another study conducted by the University of Oxford, United Kingdom on Pharmacological modulation of pain-related brain activity during normal and central sensitization states in humans, the PET and FMRI studies found deactivations in the posterior cingulate cortex, precuneus, retrospenial cortices, ventral and dorsal medial prefrontal cortex.

In the part 2, the analysis was done to prove that pain habituation exists and that inducing repetitive stimuli will show pain adaptation of the signal and that the activations of the pain will reduce with respect to time. This concept was proved in our study when

we saw reduced activations in 20-28 second duration when the first two blocks of the pain stimuli protocol were compared to the last two blocks of the pain stimuli protocol.

These findings were found to be similar to a study conducted by Meryem Yucel, where they found pain habituation symptoms in a short interval out of the first three minutes of the stimulus when innocuous and noxious stimuli were induced in the subjects [23]. The hemodynamic response of 13 out of the 60 channels were found to be significantly different in the 20- 28 second duration showing symptoms of pain adaptation between the first two blocks and the last two blocks.

Our results proved to be consistent with various other studies conducted on pain adaptation. Marieke Jepma performed an experiment in which repeated thermal stimulation on the same skin site produced habituation when a sequence of 24 repeated stimuli for 12 seconds each was applied to the subjects on the volar surface of participants' left inner forearms, using a 16 × 16 mm Peltier thermode and repeated stimulation across different skin sites produced sensitization in which the stimulation sites were changed adjacently in a series [19]. There have been reports of substantial decrease in thermal pain following a slight decrease in thermal temperature [21]. Researchers from the University of Hamburg (UKE), Germany found significantly decreased activity related to painful thermal stimulation on day 8 compared to day 1 in several sites of the pain matrix, including the medial thalamus, the anterior insula bilaterally, contralateral SII and bilateral putamen [22].

In another research study conducted by the Irani Farzin and colleagues, innocuous and noxious electrical stimuli was induced and hemodynamic changes were observed in somatosensory cortex and pain habituation effects were noticed. The possible explanation given was that nociceptors transform noxious stimuli into electrical signals

and these are then transferred to the central nervous system. Pain is inhibited to higher cortical regions by descending inhibition of higher cortical regions that contain opioid receptors. If painful stimuli cannot be avoided in favor of superior goal, anti-nociceptive mechanisms are activated by cognitive centers of brain. This plays a role in habituation of the stimuli [14].

Due to their periodic nature, block design experimental protocols result in habituation which may affect anticipation. Hence, further work is necessary to experimentally test for habituation by incorporating event-related or mixed design protocols.

Chapter 5

Conclusion and Future scope

After performing this study, we came across a few limitations that needed to be addressed for getting better results. A few of them include, area of study restricted to pre-frontal cortex, in probe configuration, BMPFC was neglected due to shortage of fibers, and FNIRS cannot measure all areas of the pain matrix which includes deeper layers of the brain. Also, our results were not consistent to a similar study conducted in our lab before where in activations were found in dorsolateral PFC and Anterior PFC (BA 8,9,10,44,45,46) during stimulus duration. Also, increasing the sample size would help get more significant statistical power. Selected features used in pain classification might have been too specific or restrictive e.g., thermal stimuli on the right arm. Another possible implementation would be co-registering the optodes with a human brain template in order to better localize the pain-stimulated cortical regions with a good spatial resolution. This could avoid possible displacement of the probe during the digitizer measurements. We can conclude by saying that Pre-frontal cortex area of the brain is an important area in pain processing and pain perceptions. Dorsolateral PFC and Anterior PFC, particularly play an important role in pain processing, can be used as biomarker location. These areas also plays an important role in studying pain habituation caused by repetitive stimuli. We can also state that FNIRS is a possible imaging technology that can be used for studying pain in future, while a few limitations of the technology need to be overcome.

Bibliography

1. Scholkmann, Felix, and Martin Wolf. "General Equation for the Differential Pathlength Factor of the Frontal Human Head Depending on Wavelength and Age." *J. Biomed. Opt Journal of Biomedical Optics*18.10 (2013): 105004. Web.
2. Terman GW, Bonica JJ. Spinal mechanisms and their modulation. In: Loeser JD, Butler SH, Chapman CR, Turk DC, eds.Bonica's Management of Pain . 3rd ed. Philadelphia, Pennsylvania, USA: Lippincott Williams and Wilkins; 2003:73
3. Axelrod FB, Hilz MJ. "Inherited Autonomic Neuropathies." *Seminars in Neurology Semin Neurol* 23.4 (2003): 381-90. Web.
4. Price, Donald D., and Ronald Dubner. "Mechanisms Of First And Second Pain In The Peripheral And Central Nervous Systems." *J Invest Dermatol Journal of Investigative Dermatology* 69.1 (1977): 167-71. Web.
5. Dubin, Adrienne E., and Ardem Patapoutian. "Nociceptors: The Sensors of the Pain Pathway." *Journal of Clinical Investigation J. Clin. Invest.*120.11 (2010): 3760-772. Web.
6. Hart, Robert P., James B. Wade, and Michael F. Martelli. "Cognitive Impairment in Patients with Chronic Pain: The Significance of Stress."*Current Science Inc Current Pain and Headache Reports* 7.2 (2003): 116-26. Web.
7. "Relieving Pain in America: A Blueprint for Transforming Prevention, Care, Education, and Research." *Choice Reviews Online* 49.11 (2012): n. pag. Web.
8. Holper, Lisa, Andrea Gross, Meier, Ursula Wolf, Martin Wolf, and Sabina Hotz-Boendermaker. "Physiological Effects of Mechanical Pain Stimulation at the Lower Back Measured by Functional Near-infrared Spectroscopy and Capnography." *Journal of Integrative Neuroscience J. Integr. Neurosci.*13.01 (2014): 121-42. Web.

9. Yennu, Amarnath, Fenghua Tian, Hanli Liu, Rohit Rawat, Michael T. Manry, and Robert Gatchel. "A Preliminary Investigation of Human Frontal Cortex Under Noxious Thermal Stimulation Over the Temporomandibular Joint Using Functional Near Infrared Spectroscopy." Journal of Applied Biobehavioral Research 18.3 (2013): 134-55. Web.
10. Tracey, Irene. "Nociceptive Processing in the Human Brain." *Current Opinion in Neurobiology* 15.4 (2005): 478-87. Web.
11. Friebel, Ulrike, Simon B. Eickhoff, and Martin Lotze. "Coordinate-based Meta-analysis of Experimentally Induced and Chronic Persistent Neuropathic Pain." *NeuroImage* 58.4 (2011): 1070-080. Web.
12. Groves, Philip M., and Richard F. Thompson. "Habituation: A Dual-process Theory." *Psychological Review* 77.5 (1970): 419-50. Web.
13. Gagnon, Louis, Meryem A. Yücel, and David A. Boas. "Further Improvement in Reducing Superficial Contamination in NIRS Using Double Short Separation Measurements." *NeuroImage* 85 (2014): 127-35. Web.
14. Irani, Farzin, Steven M. Platek, and Scott Bunce. "Functional Near Infrared Spectroscopy (fNIRS): An Emerging Neuroimaging Technology with Important Applications for the Study of Brain Disorders." *The Clinical Neuropsychologist* 21.1 (2007): 9-37. Web.
15. Hart, Robert P., James B. Wade, and Michael F. Martelli. "Cognitive Impairment in Patients with Chronic Pain: The Significance of Stress."*Current Science Inc Current Pain and Headache Reports* 7.2 (2003): 116-26. Web.
16. Kong, Jian, Marco L. Loggia, and Carolyn Zyloney. "Exploring the Brain in Pain: Activations, Deactivations and Their Relation." *Pain* 148.2 (2010): 257-67. Web.

17. Devor, A., P. Tian, and N. Nishimura. "Suppressed Neuronal Activity and Concurrent Arteriolar Vasoconstriction May Explain Negative Blood Oxygenation Level-Dependent Signal." *Journal of Neuroscience* 27.16 (2007): 4452-459. Web.
18. Wiech, Katja, Markus Ploner, and Irene Tracey. "Neurocognitive Aspects of Pain Perception." *Trends in Cognitive Sciences* 12.8 (2008): 306-13. Web.
19. Jepma, Marieke, Matt Jones, and Tor D. Wager. "The Dynamics of Pain: Evidence for Simultaneous Site-Specific Habituation and Site-Nonspecific Sensitization in Thermal Pain." The Journal of Pain 15.7 (2014): 734-46. Web.
20. Groves, Philip M., and Richard F. Thompson. "Habituation: A Dual-process Theory." Psychological Review 77.5 (1970): 419-50. Web.
21. Bingel, U., E. Schoell, and W. Herken. "Habituation to Painful Stimulation Involves the Antinociceptive System." *Pain* 131.1 (2007): 21-30. Web.
22. Derbyshire, S. W., A. K. Jones, and P. Devani. "Cerebral Responses to Pain in Patients with Atypical Facial Pain Measured by Positron Emission Tomography." *Journal of Neurology, Neurosurgery & Psychiatry* 57.10 (1994): 1166-172. Web.
23. Yücel, Meryem A., Christopher M. Aasted, and Mihayl P. Petkov. "Specificity of Hemodynamic Brain Responses to Painful Stimuli: A Functional Near-infrared Spectroscopy Study." *Sci. Rep. Scientific Reports* 5 (2015): 9469. Web.

.

Biographical Information

Koumudi Chari graduated from Vidyalankar Institute of Technology, Mumbai, India in 2012 with Bachelor's degree in Biomedical Engineering. She joined UT Arlington in fall 2013 to pursue Master's degree. After having undertaken courses on Medical Imaging, Tissue Optics and Advanced Neuro Imaging, she commenced her research on Pain study using FNIRS imaging technology.